Mining of Mineral Deposits
Volume 19 (2025), Issue 1, 82-97

MMD JOURNAL / MINING.IN.UA

https://doi.org/10.33271/mining19.01.082

Development and implementation of active and combined support types for sections of mine workings exposed to bearing pressure

Assylbek Abdirashit [1], Zhadyrassyn Sarkulova [1*], Marat Imangazin [1*], Riza Orazbekova [1], Gulya Issengaliyeva [1], Kulzhamal Nauryzova [1], Gulnara Bimagambetova [2]

[1] *K. Zhubanov Aktobe Regional University, Aktobe, Kazakhstan*
[2] *Kazakh-Russian International University, Aktobe, Kazakhstan*

Corresponding author: e-mail zh.sarkulova@zhubanov.edu.kz, mimangazin@zhubanov.edu.kz

Abstract

Purpose. The research aims to develop and substantiate an effective technology for supporting mine workings in conditions of complex geomechanical and hydrogeological factors based on the analysis of data on the border mass strain state, the effectiveness of the supports used, as well as the behavior of materials and structures in the process of operation.

Methods. The research includes the use of endoscopic surveys of wells to diagnose the border mass for the purpose of identifying fractures, cleavages and other zones of weakening. The tests are conducted on the roof-bolting support including AK01-21N(U) and AK01-30PN rope bolts with a tension of up to 100 kN. Two-component resin (15 liters per blast-hole) and DAK-1-500 N resin capsules are used for complete filling of the blast-holes. In addition, the properties of MasterRock STS 1510 shotcrete support are studied with dynamic strength control.

Findings. The border mass deformations have been revealed, including fracture opening up to 1.6 m, caused by the presence of ore inclusions. The use of roof-bolting support with full filling of blast-holes with two-component resin and resin capsules has shown high efficiency. The AK01-30PN rope bolts with a tension of up to 100 kN have provided significant increase in the mass stability. MasterRock STS 1510 shotcrete has shown satisfactory strength characteristics. Minor fractures have been detected that do not influence the overall stability of the mine workings.

Originality. The patterns of the border mass deformation behavior under conditions of complex geomechanical factors, including zones of fracturing and local weakening caused by ore inclusions, have been revealed and characterized. It has been found that complete filling of blast-holes with two-component resin and resin capsules for reinforcing rope bolts provides a significant increase in the mass stability. The integrated use of roof-bolting and shotcrete support has proven to be effective in reducing the impact of water inrush and increasing the strength characteristics of mine workings.

Practical implications. The developed technology for supporting mine workings using rope bolts with tension up to 100 kN and full filling of blast-holes with two-component resin can be implemented at mining enterprises, which will increase the stability of mine workings and safety of operations in conditions of complex geomechanical factors. The results of endoscopic diagnostics and monitoring of the border mass deformations provide a tool for timely identification of weakening zones and taking measures to strengthen the support, contributing to increased efficiency during mine working operation.

Keywords: *stress state, mass, ore, rock, well, support, Barton's Q-index*

1. Introduction

The mining industry of Kazakhstan, thanks to its natural resources, occupies a strategically important place in the economy of the country, providing a significant share of exports and being the main source of raw materials for many industries [1], [2]. In particular, Kazakhstan is known for its reserves of coal, copper, gold, uranium and other minerals, making it one of the leading producers in the world market [3]-[6]. However, as mining depth increases and the mining of more complex and hard-to-reach deposits becomes more challenging, the need to address such issues as safety in mining operations, ensuring the mine working stability, and improving the efficiency of natural resource use increases. These issues are of particular importance in light of increasing requirements for environmental standards and optimization of production processes [7].

In recent years, research has focused on optimizing mining operations through data-driven approaches and advanced computational methods. For instance, the development of data classification systems for local administration has been proposed to enhance decision-making processes in the mining sector, contributing to improved resource management and operational efficiency [8], [9]. Additionally, modern machine learning techniques, such as ensemble approaches combining deep residual networks with attention mechanisms, have shown promise in predictive analytics, which could be adapted to monitor and optimize mining

Received: 4 September 2024. Accepted: 20 February 2025. Available online: 30 March 2025

Mining of Mineral Deposits. ISSN 2415-3443 (Online) | ISSN 2415-3435 (Print)

operations [10]. Furthermore, the structuring and modeling of business processes play a crucial role in streamlining mining activities, ensuring better control over production workflows and resource allocation [11], [12].

With the development of mining technologies and the move to deeper horizons of deposit mining, the need to address a number of issues related to safety of mining operations and stability of mine workings becomes obvious [13]. The challenge is that deep horizons are characterized by a high stress level in the rocks, which increases the risk of caving, shearing and other hazardous phenomena influencing the efficiency and safety of operations [14]-[16]. In addition, the influence of tectonic faults and geological peculiarities of deposits requires the development of new methods and technologies to ensure the reliability and durability of mine workings, which necessitates a systematic approach based on the use of advanced methods of numerical modeling and analysis [17], [18].

Recent studies highlight the importance of considering natural stress fields and the impact of blasting forces on rock mass stability in deep mining operations. Research [19] emphasizes that understanding the stress distribution in the rock mass can significantly improve blasting efficiency and minimize unintended deformations. Similarly, research [20] proposes sectional blasting as an effective method for optimizing cut cavity formation, which enhances the stability of underground workings. Numerical modeling techniques can be utilized to assess the stress-strain state of rock masses near vertical excavations in combined mining [21]. Assess the instability of hanging wall rocks during underground iron ore mining, emphasizing the necessity of precise monitoring and preventive measures to mitigate potential rock falls and structural failures in underground excavations [22].

Practice shows that for the same conditions, it is usually possible to use different methods and technologies, which can vary significantly in their effectiveness and cost [23]-[25]. In the context of the mining industry, this is particularly relevant, as the choice of appropriate methods depends on many factors, such as the geological peculiarities of the deposit, the depth of mining, the mechanical properties of the rocks, as well as economic and environmental constraints.

When conducting mine workings at different horizons, especially at deep horizons, it is necessary to consider not only standard methods, but also adapted solutions that can be associated with the use of new technologies, innovative materials, as well as more accurate methods of predicting and modeling geomechanical processes [26], [27]. It is also important to take into account that the practical application of these technologies requires a high level of professional expertise, as well as the development of localized methods that can work effectively within the specific conditions of particular deposits [28], [29].

The purpose of this research is to develop and improve the methods for ensuring the stability of mine workings at deep horizons of mining deposits in Kazakhstan. The research plans to conduct a detailed analysis of factors influencing the stability of mine workings, as well as to study numerical modeling methods for predicting the behavior of rocks under high operational loads. Particular attention will be given to the development of effective methods for supporting and stabilizing mine workings, as well as to assessing the risks associated with possible caving and other emergency situations, and to developing recommendations for improving safety and efficiency in mining operations.

2. Study area

The 10th Anniversary of Kazakhstan's independence Mine is located in the north of Mugalzhar, on the eastern slope of the East Kempirsay ore region, in the south-eastern part of Khromtau City, Aktobe region. The Rudnichny District infrastructure is well developed. Near the 10th Anniversary of Kazakhstan's independence Mine, chromite deposits are mined by the mines of Donskoy Ore Mining and Processing Plant (a branch of TNK Kazchrome JSC) and the Voskhod Mine (Voskhod Oriel LLP). A beneficiation plant for processing of chromite ores produced at these deposits is located three kilometers north of the Molodezhnaya Mine [30], [31].

At all deposits of the South Kempirsay Region, natural types of chromite ores are distinguished by textural peculiarities and the amount of chromospinelides in them, and technological ore grades – by the content of chromium oxide and silicon.

The chromite ores' mineral composition is quite simple. The ores consist of chromospinelides and cement minerals, which are represented by serpentinite, olivine and carbonate. Noteworthy is that the lower the ore grade, the greater the serpentinite component. Ores with a chromium oxide content of more than 45% do not require beneficiation. They account for 86.7% of deposit reserves (240.2 million tons). The content of chromium oxide is 52.3% in high-grade ores and 38.9% in raw ores.

At the deposit of the 10th Anniversary of Kazakhstan's independence Mine zone, there is a significant development of serpentinites, especially through dunites, which creates unique conditions for mining operations. These rocks have different strength characteristics, which can vary considerably depending on the depth of occurrence and their mineralogical composition. The serpentinization process, as well as various geological and physical-mechanical properties of the rocks (degree of fracturing, compressive strength, and strength index according to Protodyakonov scale), become decisive in the choice of methods for deposit mining and supporting mine workings. Deeper mining at the deposit leads to the need for understanding and modeling rock behavior at different depths to assess risks and minimize the probability of caving, as well as to improve the safety of mining operations. At the deposit of the 10th Anniversary of Kazakhstan's independence Mine zone serpentinites are widespread through dunites, while through pyroxene dunites they are less common. These rocks extend from 35 to 110 m below the earth's surface. At depths of 10-20 m, the greatest manifestation of rock desiccation is observed, where they, originally fine-grained, have over time transformed into clay mass [32].

Four key engineering-geologic rock complexes have been identified during laboratory tests:

1) complex of ground carbonate fine-grained serpentinites of low strength (R_c = 15.2 MPa, R_t = 1.3 MPa, f = 2-3, drilling category III), characteristic of the upper layers of the deposit;

2) complex of serpentinized dunites:

– less fracture-resistant dunite has high strength (R_c = 55.3 MPa, R_t = 4.3 MPa, f = 9, drilling category VII);

– medium-quadratic dunite – rocks of medium strength (R_c = 27.1 MPa, R_t = 3.1 MPa, f = 8, drilling category VII);

– hard dunites (R_c = 64.5 MPa, R_t = 4.5 MPa, f = 9, drilling category VII);

– medium-maturing dunites of medium strength (R_c = 35.1 MPa, R_t = 2.7 MPa, f = 8, drilling category VII);

– ultra-high strength dunites with low strength (R_c = 17.1 MPa, R_t = 1.6 MPa, f = 6, drilling category VI);

3) complex of serpentinized peridotites:

– low tensile strength rocks (R_c = 58.1 MPa, R_t = 4.7 MPa, f = 8, drilling category VII);

– medium strength rocks (R_c = 29.1 MPa, R_t = 2.7 MPa, f = 8, drilling category VII);

– ultra-high tensile strength rocks (R_c = 8.0 MPa, R_t = 0.8 MPa, f = 2, drilling category III).

Rock strength increases with depth, and the compressive strength of low-tonnage rocks and ores at great depths can range from 60 to 120 MPa.

The main ore deposit consists mainly of continuous and densely disseminated ores, and the rocks are represented by varying degrees of serpentinization: pyroxene-free dunites, pyroxene dunites and peridotites.

A general view of the face at the time of the transfer of mine working is presented in Figure 1.

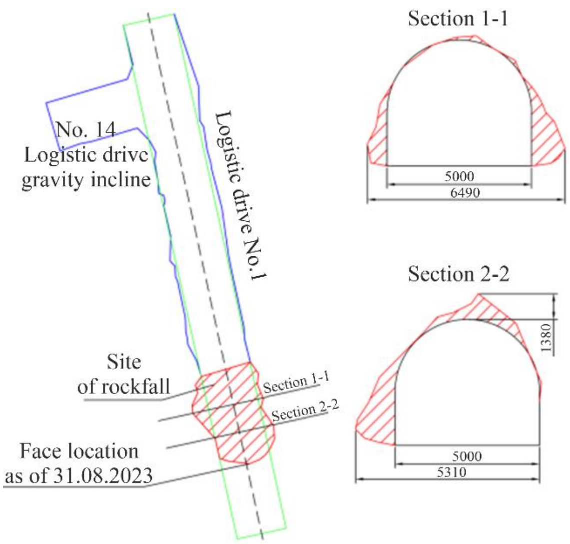

Figure 1. Sketch of rockfalls in the tectonic fault zone

Figure 1 shows a graphical interpretation of the face at the time of the mine working transfer at the site of mining facility, with an emphasis on the area exposed to tectonic faulting.

General view of the face indicates the current location of the mine working and its parameters as of August 31, 2023. The face is characterized by a clear identification of the mutual location of the tunneling working relative to geological structure, and also implies integration with project data on drilling and supporting. The tectonic fault zone shown in the sketch represents an area of altered geologic structure where active shears, faults or other tectonic disturbances are present that influence the strength characteristics of rocks and potentially increase the risks associated with mining-tunneling operations. In this area, there may be changes in rock stability and increased requirements for engineering solutions in terms of strengthening tunnels and other underground structures.

Tunneling operations at the experimental site of logistic drive No. 1 are conducted in the rock with a medium strength of 30-60 MPa, which is a favorable factor compared to the conditions of logistic drive No. 9 gravity incline. Figure 2 shows a general view of the face during mining-tunneling operations at the experimental site of logistic drive No. 1.

Tunneling operations at the experimental site of logistic drive No. 1 are conducted in medium-strength rocks with the ultimate strength of 30-60 MPa, which creates relatively favorable conditions for tunneling, but requires the use of reliable methods of supporting to prevent caving and ensure the rock mass stability. At the initial stage of tunneling, there is a significant loosening of rock and local caving caused by redistribution of stresses in the mass. The face state at this stage demonstrates significant border zone destruction and fragmentary displacements of rock blocks (Fig. 2a). The use of primary supporting elements makes it possible to localize the failure zone and prevent further development of deformations.

At the next stage, after setting temporary supporting elements, stabilization of the face structure is observed. The main deformation is concentrated in the border zone, while the central face part remains relatively stable (Fig. 2b). The use of mesh coverings and roof-bolting systems reduces the risk of subsequent caving and provides pre-strengthening of the rock mass. The strengthening process continues, and at later stages, an improvement in the face stability is observed. The setting of roof-bolt supporting elements and frame structures creates additional strengthening necessary to prevent displacement in weak areas (Fig. 2c). During this period, the focus is on controlling the state of the face walls and point stabilization of the zones most prone to deformation. At a depth of 12 l.m (Fig. 2d), the supporting process is nearly complete. The use of durable roof-bolting systems and steel spacers ensures long-term stability of the face and creates safe conditions for the operations to continue. By this time, visible deformations are minimized and the risk of localized caving is significantly reduced.

At subsequent stages, the strengthening is supplemented by setting of permanent supporting elements aimed at redistributing the loads in the rock mass. Additional strengthening measures using metal elements and geopolymer materials provide reliable stabilization of the face walls (Fig. 2e). The final stage (Fig. 2f) is characterized by the full completion of the stabilization process. Permanent supporting elements are set to ensure rock stability and minimize the risk of further deformation.

3. Methodology

Surveys and observations of the actual state of the mine working – logistic drive No. 1at hor. -175 m of the 10th Anniversary of Kazakhstan's independence Mine -1 during experimental and industrial testing at the experimental site was conducted over a length of 30 l.m from 25.07.2023 to 20.11.2023. According to the technical specification after the transfer of mine working for the conduct of experimental and industrial tests, geotechnical monitoring was carried out at the experimental site. Monitoring was performed in accordance with the "Methodology for conducting geotechnical monitoring of the state of border and support of experimental sites at the 10th Anniversary of Kazakhstan's independence Mine -1 of Donskoy Ore Mining and Processing Plant – a branch of TNK Kazchrome JSC".

Geotechnical assessment of the state of the experimental site of logistic drive No. 1 at hor. -175 m of the 10th Anniversary of Kazakhstan's independence Mine -1 was conducted from the moment of transferring the mine working for experimental and industrial tests. Monitoring was conducted all the time.

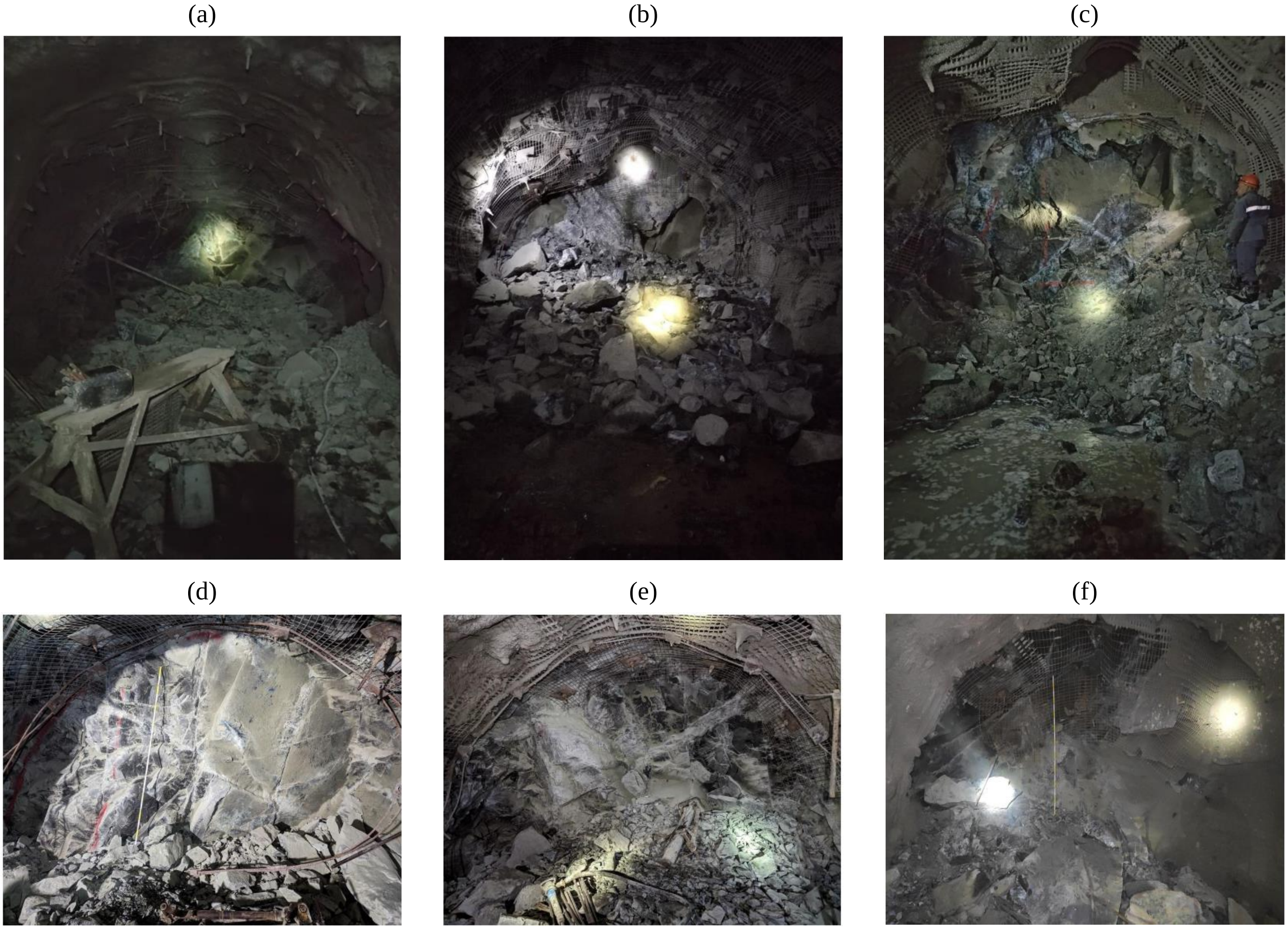

Figure 2. A general view of the logistic drive No. 1 face at the time of supporting: (a) 3 l.m; (b) 6 l.m; (c) 9 l.m; (d) 12 l.m; (e) 14 l.m; (f) 16 l.m

During the assessment, the rating of the rock mass by RMR (Rock Mass Rating) by Z.T. Beniavsky, Barton's Q-index, the index of rock mass disturbance by fractures (Rock Quality Designation (RQD), the uniaxial compression strength of the rock – (UCS) and the stability categories of the mass were determined. Visual inspections of the experimental site state were also made. The results are presented in Table 1.

Measurement of uniaxial compression strength (UCS) characteristics of rocks was performed by means of an express method based on shock pulse, using an electronic sclerometer ONIKS-2.5. This method provides a rapid assessment of the mechanical properties of the rock directly in the field conditions. To improve the accuracy of determination of strength characteristics, the samples are also taken with subsequent laboratory testing of their mechanical properties on the device of concentrated loading PSN-0.16.10. This integrated approach provides a more reliable assessment of strength characteristics, which is critical for geomechanical calculations and predicting the stability of rock masses.

Table 2 presents the parameters by which the RMR by Z.T. Beniavsky and Barton's Q-index are determined.

Table 1. Summary data on mine working and mass properties

Experimental site, l.m	RMR	*Q*	Category of stability	RQD, %	UCS, MPa	Note
1, 2	36	0.165	IV (unstable rocks)	61	54	When setting the roof-bolting support, water inrush in the form of dripping is fixed in the roof, which has a negative effect on stability.
3, 4	21	0.079	V (highly unstable rocks)	37	35	
5, 6	19	0.076		35	40	
7, 8	20	0.081		33	35	Activities undertaken: – drainage wells are drilled in the roof to reduce the negative impact of water on shotcrete; – from 3 to 12 l.m, there is an intensive cutter break formation and sliding of separate blocks along the roof and walls. On the left and right walls of the site during rock mass shipment – local rockfalls up to 0.3 m deep occur along the surface of slip joints.
9, 10	21	0.078		35	45	
11, 12	21	0.080		35	35	
13, 14	35	0.15	IV (unstable rocks)	57	45	
15, 16	36	0.14	V (highly unstable rocks)	55	49	
17, 18	43	0.21	IV (unstable rocks)	60	55	
19, 20	42	0.22		58	53	
21, 22	38	0.19		55	52	
23, 24	40	0.20		53	44	
25, 26	37	0.16		52	45	
27, 28	41	0.22		53	60	
29, 30	36	0.18		55	55	

Table 2. Parameters for determining the RMR by Z.T. Beniavsky and Barton's Q-index at the experimental site of logistic drive No. 1at hor. -175 m of the 10th Anniversary of Kazakhstan's independence Mine -1 (1-16 m)

Experimental site of logistic drive No.9 gravity incline, l.m			1-2	3-4	5-6	7-8	9-10	11-12	13-14	15
Mine working width, m			4.67	5.09	5.12	4.98	4.80	4.91	4.87	4.89
A1	Degree of fracturing (by primary system)	Uniaxial compression strength (UCS), MPa	4.45	4.42	4.89	5.17	5.21	5.11	5.13	5.08
B1			60	52	45	30	20	25	30	25
B4		RQD, % – index of rock mass disturbance by fractures (sum of fracture lengths with a spacing of more than 10 cm per 1 m)	62	59	52	25	24	24	30	24
C1	Structure of fracturing (by primary system)	Block shape: a – cube-shaped block; b – slightly long and flat block; c – moderately long and flat block; d – very long and flat block	c	c	c, d	d	c, d	c, d	c	c, d
C2		Fracture systems: a – no; b – 1 system; c – 1 system + random; d – 2 systems; e – 2 systems + random; f – 3 systems; g – 3 system + random; i – fragmented	a	a, b	a	a, c	a, c	a, b	a	a, b
C3		Orientation relative to the main fracture system: a – very favorable; b – favorable; c – moderately; d – unfavorable; e – very unfavorable	f	g	g	g, i	g, i	g, i	g	g
C4			roof	c	c	c	d	c	c	c
			wall	d	d	d	d	d	d	d
D1	Fracture roughness	Fracture micro-roughness: a – step-like; b – rough; c – slightly rough; d – mooth; e – polished; f – slickensided surface	d	c	d	f	f	f	f	f
D2		Fracture waviness: a – choppy; b – strongly wavy; c – medium-wavy; d – slightly wavy; e – flat (with smooth friction clay); f – slickensided surface	d	e	d	f	d, f	f	f	f
D3	Alteration and weathering	Without filler: a – closed; b – clean / no filler; c – slightly altered; d – altered; e – covered with sand/silt; f – coated with talc-like hydrophilic minerals	c	f	f	f	b, f	b, f	f	f
D3	Alteration and weathering	Filler < 5 mm: h – strong minerals; j – serpentinite; i – soft minerals; n – talc-like minerals (serpophite)	n	i	n	n	j, n	j, n	n	n
		Filler > 5 mm: i – strong minerals; k – serpentinite; m – soft minerals; o – talc-like minerals	k	k	k	m, o	k, o	k, o	o	o
D4	Fracture length: a – continuous mass; b – discontinuous; c – very short (0.1-1 m); d – short (1-3 m); e – medium (3-6 m); f – long (6-10 m); g – fault (if a fault system is mapped)		e	c, d	d	d, e	d	d, e	e	d, e
D5	Fracture opening: a – no; b – very narrow (< 0.1 mm); c – narrow (0.1- 0.5 mm); d – moderately open (0.5-2.5 mm);e – open (2.5-10 mm)		e	e	d, e	d, e	d	d	d	c, d
E	Adhesion or compactness of the rock mass structure: a – very dense; b – dense or compact; c – disturbed; d – poor continuity (decompacted with soil-like rock inclusions)		c	c	c	c, d	c, d	c, d	c	c
F	Water inrush: a – dry or moist; b – moist; c – wet; d – dripping; e – mean water inrush; f – high water inrush		d	d	c	a, b	a	a	a	b
G1	Stress level: a – very low stresses; b – low stresses; c – medium/moderate stresses; d – high stresses		c	b	b	b	b	b	b	b
D3	Superlimiting stresses	Rock outburst or rock bump: e – exfoliation; f – rock outburst; g – rock bump	–	–	–	–	–	–	–	–
		Pressing-out: h – medium degree; i – strong degree	h	h	h	h	h	h	h	h

Thus, the analysis of rock mass parameters at the experimental site of logistic drive No. 1 at hor. -175 m of the 10th Anniversary of Kazakhstan's independence Mine -1 within 1-16 m shows significant variability in the characteristics determining the RMR-Beniavsky and Barton's ratings. Rock strength (UCS) ranges from 4.42 to 5.21 MPa, the degree of fracturing decreases with depth, and the RQD index ranges from 24 to 62%, reflecting varying degree of rock mass disturbance. The fracture structure is predominantly represented by moderately long and flat blocks with one or two major fracture systems, their orientation varying from favorable to unfavorable. The roof of the site is mostly stable, while the walls are characterized by reduced stability. The roughness and waviness of the fractures are variable, with a predominance of smooth and polished surfaces. Fracture fillers contain soft minerals, including talc-like formations, which reduces the strength characteristics of the mass. The fractures are mostly medium in length (3-6 m), the opening is moderate (0.5-2.5 mm), and the rock mass structure varies from dense to disturbed. Water inrush is mostly weak, but dripping is noted at some points. The stress state of the mass is mainly characterized by low and moderate levels, with the manifestation of medium degree pressing-out of rocks, which indicates the need for additional measures to strengthen the rock mass during mining.

Control over rock displacement using reference depth markers (RDM) allows for effective monitoring of deformation processes in the mass. These devices record vertical and horizontal displacements of rock layers, which allows for timely identification of high-stress zones and prediction of possible caving.

Two RDM measuring stations were set to determine the intensity of displacements and cleavages of the roof rocks at the experimental site:

– RDM measuring stations No.1 at the experimental site of logistic drive No.1 was set in the roof along the axis of the mine working, between the 8th and 9th rows of support (8.5 m from the boundary of the beginning of the experimental site);

– RDM measuring stations No. 2 at the experimental site of logistic drive No. 1 was set in the roof along the axis of the mine working, between the 21st and 22nd rows of support (22.5 m from the boundary of the beginning of the experimental site);

Layout of reference points for the measuring stations and the depth of their setting are presented in Figure 3. The RDM photo is presented in Figure 4.

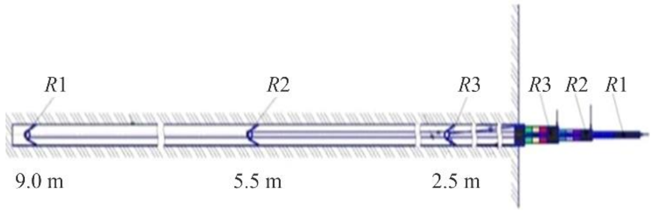

Figure 3. Layout of reference points for RDM measuring stations and the depth of their setting

Figure 4. General view of the RDM measuring stations after setting

The use of reference depth markers (RDM) provides high accuracy for monitoring deformation processes in rocks, allowing timely identification of potentially dangerous areas and taking measures to strengthen mine workings. Due to the RDM measuring stations set at the experimental site and the organized systematic monitoring of changes in the position of the roof rock, it became possible to improve the safety of mining operations and reduce the risks of accident situations. Further use of the RDM control methodology allows for statistical data to be collected for better prediction and optimization of the supporting systems in the conditions of a particular deposit.

4. Results and discussion

4.1. Geological assessment of the experimental site

The experimental site is located in zone III of the tectonic fault and the Buka Zapad tectonic fault, as well as in the ore contact zone. Average rock strength is 30-60 MPa. In this regard, tunneling operations are complicated: the mass is characterized as highly fractured from unstable to very unstable, and fractures are filled with talc-like minerals, the surfaces of which are represented by slickensided surfaces (IV and V category of stability). The results of geological assessment of the experimental site of logistic drive No. 1 are shown in Figure 5.

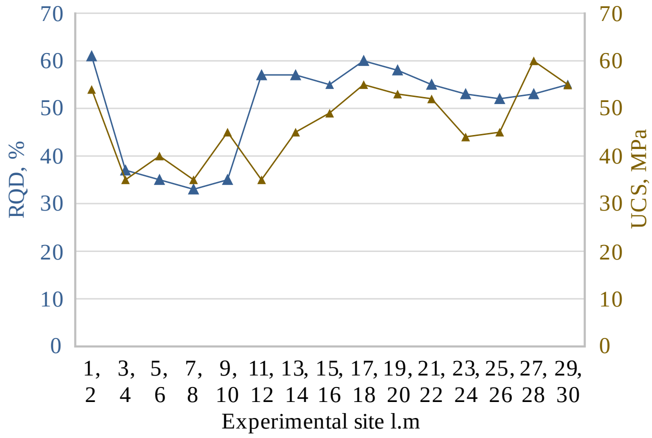

Figure 5. Changes in RQD and UCS along the length of the experimental site, l.m

During the period of tunneling operations, water inrush is observed from the overlying horizon through the fracture systems, manifested in the form of local dripping, which also influences the decrease in stability. After strengthening the experimental site, there is no dripping, but localized wetting of shotcrete is observed.

The mass is strongly fractured, and the fractures are filled with talc-like minerals, accompanied by slickensided surfaces. During driving, there is water inrush in the form of dripping, which negatively influences stability. The mass is weak, unstable. When a fracture junction is opened, sliding of individual blocks occurs.

4.2. Assessment of cleavage and fracture zones using video-endoscopic survey

The primary assessment of cleavage and fracture zones using video-endoscopic survey of the border mass was conducted at 10 m of the experimental site of logistic drive No.1.

Well No. 1 of ∅32 m and 9.31 m depth was drilled into the roof of logistic drive No. 1, at a distance of 10 m from the beginning of the experimental site, for subsequent RDM setting. The geomechanical state of the wellbore is presented in Figure 6. The images record the rock state at different depths, which allows a detailed analysis of the nature of fracturing, weakened zones and stable rock mass areas.

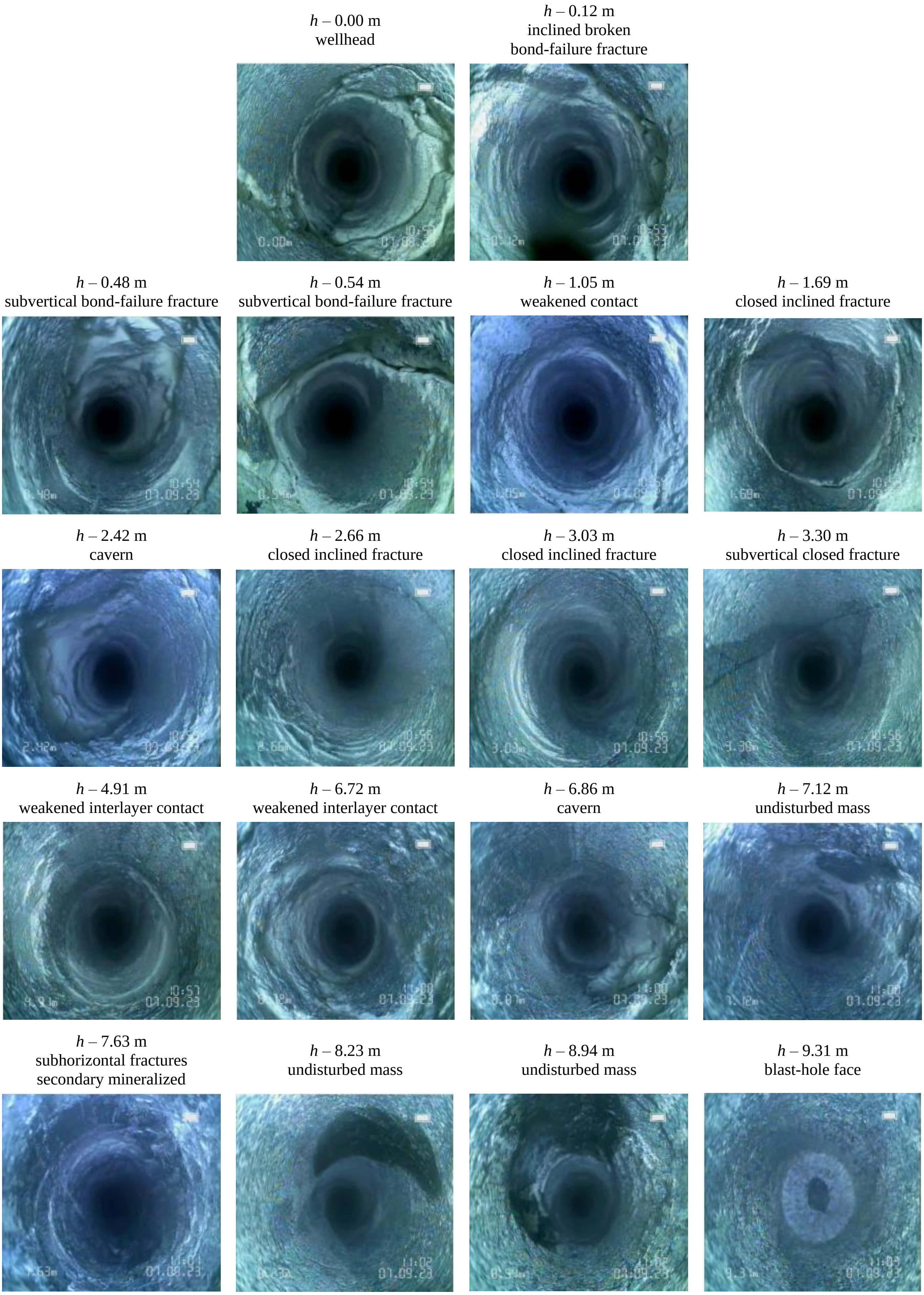

Figure 6. Survey of the wellbore No.1 geomechanical state

At initial depths, there are minimal disturbances in the rock mass structure, which is characteristic for the surface and upper rock layers (Fig. 6, h = 0.00 m). However, already at a depth of 0.12 m, an inclined broken bond-failure fracture is identified, probably formed as a result of local geodynamic processes. This fracture may indicate the presence of localized stresses in the rocks, which requires further observation and analysis.

At depths of 0.48 and 0.54 m, subvertical bond-failure fractures are recorded, indicating vertical rock mass disturbances. Such fractures can significantly reduce the strength and stability of the rock base. At a depth of 1.05 m, there is a weakened contact between the rock layers, indicating a decrease in the adhesion of the rock layers. At the same time, closed inclined fractures, found at depths of 1.69, 2.66 and 3.03 m, indicate partial restoration of the mass continuity. The mentioned areas retain relative stability.

Caverns are noted at 2.42 and 6.86 m depths. Such cavities in the rocks are an indicator of material leaching. The presence of caverns increases the risk of instability. At depths of 4.9 and 6.72 m, weakened interlayer contacts are identified. Such zones often become localized displacement foci and pose a potential hazard to well stability.

In the range of 7.12-8.94 m, the rocks remain relatively undisturbed, indicating the stability of the mass at these depths. Such an area is characterized by the absence of significant geological faults and minimal signs of fracture formation. The maximum well depth (9.31 m) corresponds to the face, where the rock structure remains intact and stable.

The presented video-endoscopic survey results (Fig. 6) demonstrate the presence of both disturbed and stable areas. This approach allows a detailed assessment of the geomechanical state of the well, as well as the identification of potentially hazardous zones.

Subsequent assessment of the presence of cleavage and fracture zones using video-endoscopic survey method of the border mass was conducted at 20 and 10 m levels of the experimental site of logistic drive No. 1. Two wells of ∅32 mm were drilled at 20 m level of the experimental site. Well No. 2, 8.49 m deep, was drilled into the roof, and well No. 3, 4.9 m deep, was drilled into the left side of the mine working.

At the 10 m level of the experimental site, 2 wells of ∅32 mm were also drilled. Well No. 4, 8.49 m deep, was drilled into the roof, and well No. 5, 5.0 m deep, was drilled into the left side of the mine working. Layout of wells and reference stations is presented in Figure 7.

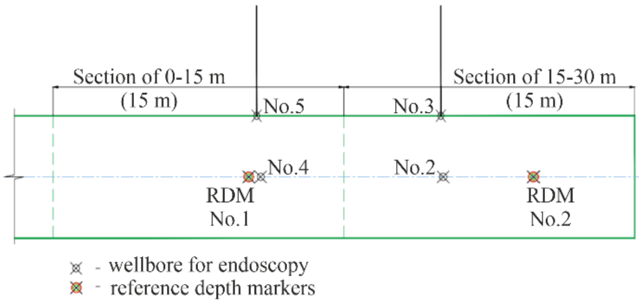

Figure 7. Layout of measuring stations and wells for video-endoscopic sounding of the mass (plan view)

The geomechanical state of the wellbore is presented in Figure 8. The images record the rock state, identifying stable areas, zones of weakening and disseminations of ore bodies that can significantly influence the well stability.

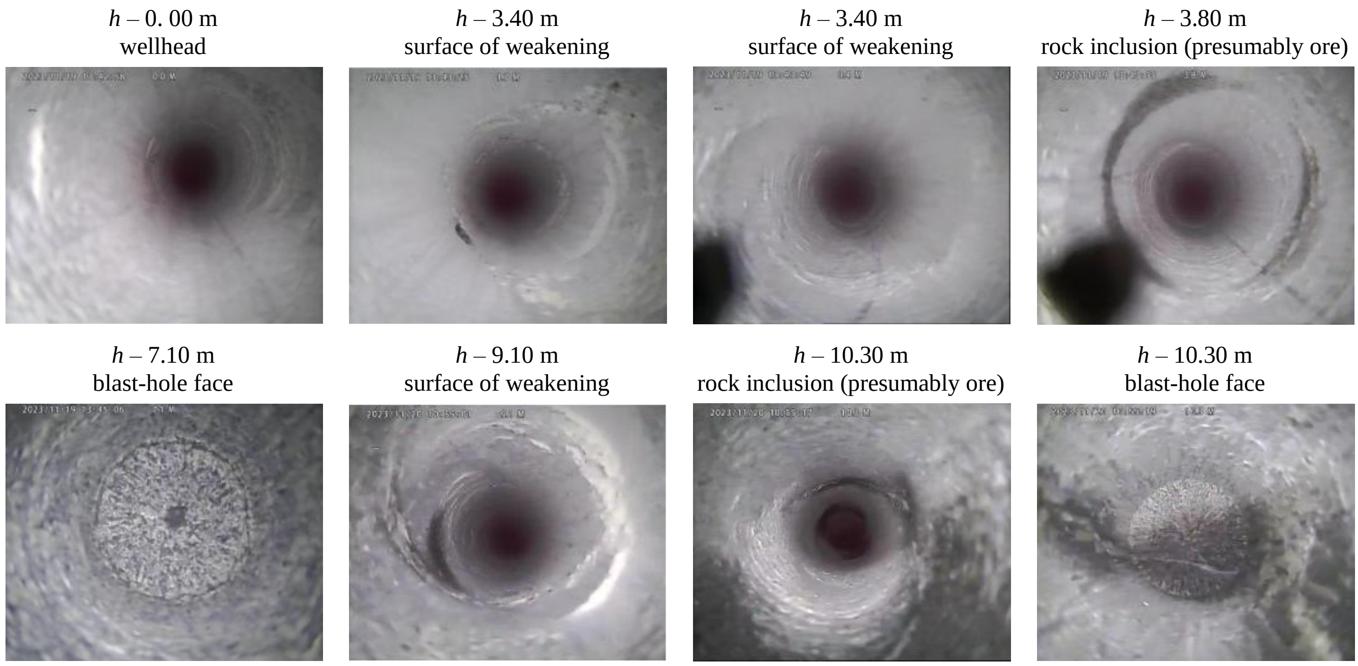

Figure 8. Survey of the wellbore No. 2 geomechanical state

At the initial level, in the wellhead (Fig. 8, h = 0.00 m), the mass state appears stable, with no visible signs of fracturing or weakening. The upper rock layers retain their continuity, indicating the normal state of the border zone.

At a depth of 3.40 m, there is a surface of weakening. Such surfaces may be the result of localized fractures or deformation processes that reduce the strength of the rock mass. Repeated fixation of a weakened surface at the same depth indicates the presence of repetitive structural disturbances. At a depth of 3.80 m, there is rock dissemination presumably of ore origin. The presence of ore bodies can alter the physical-mechanical properties of the rock, creating localized areas of increased or decreased strength. The blast-hole face at a depth of 7.10 m is represented as a zone with a relatively stable rock state. There are no visible signs of fractures or deformations at this level. At 2 m deeper (*h* = 9.10 m), the surface of weakening is again fixed, confirming the presence of weak areas prone to further displacement or deformation. The surface of weakening is nothing more than a potentially dangerous zone, especially under the influence of external loads. At 10.30 m level, there is a second rock dissemination similar to the previously recorded one. The dissemination is probably associated with mineralized zones. At the final depth, there is a stable state of the wellbore.

Figure 9 presents photos of video-endoscopic survey of wellbore No. 3, during which changes in the geomechanical state of the mass at different depths are recorded.

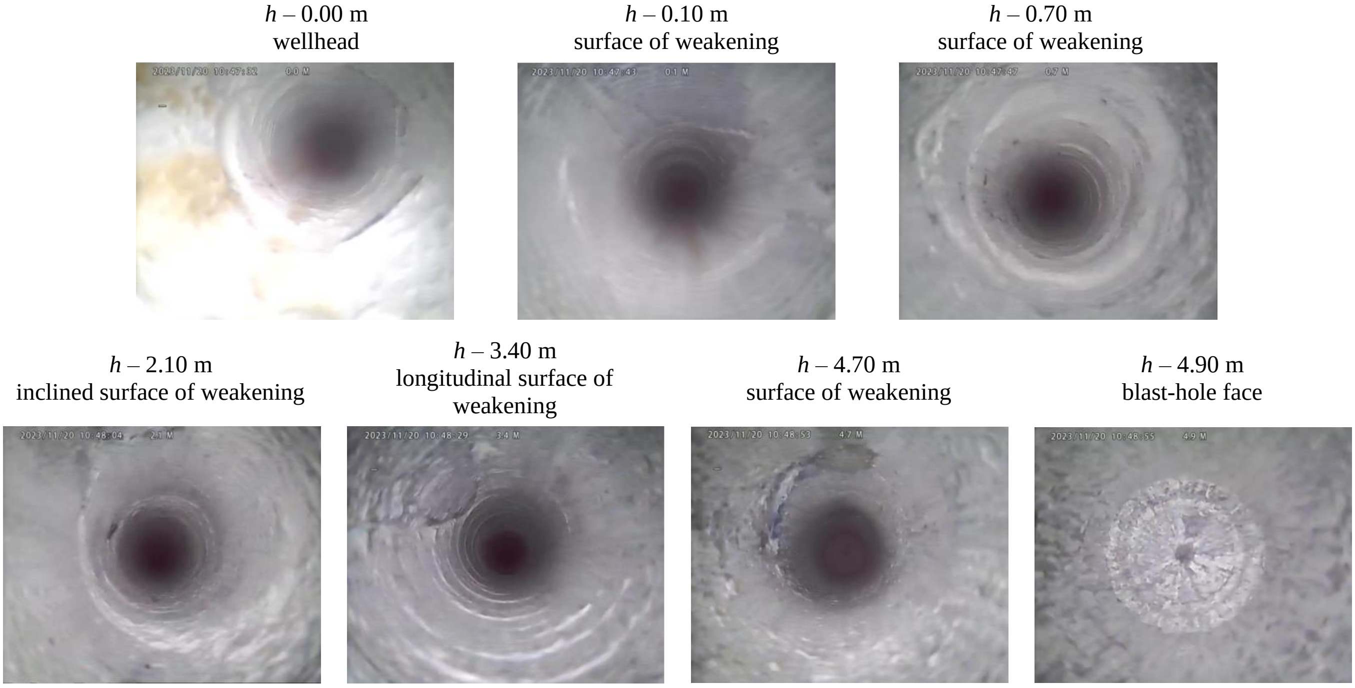

Figure 9. Survey of the wellbore No.3 geomechanical state

The video-endoscopic survey indicates both stable areas and zones of weakening that require further analysis to prevent possible deformations. At the initial level, in the wellhead (Fig. 9, *h* = 0.00 m), the mass state is assessed as stable, without significant deformation or failures. Surfaces at this level retain continuity, which is characteristic of the upper rock layers. At a depth of 0.10 m, there is a surface weakening, which may be the first sign of incipient fracture formation. The continuation of the zone of weakening is observed at a depth of 0.70 m, which indicates the presence of zones with reduced strength in the border part of the mass.

At a depth of 2.10 m, an inclined surface of weakening is noted. Inclined fractures or disturbances of this type pose an increased risk as they can lead to localized caving and reduced wellbore stability. Longitudinal weakening at 3.40 m depth may indicate systemic disturbances that propagate along the well axis. Deeper, at 4.70 m, a further widening of the zone of weakening is observed, indicating structural changes in the rock. Blast-hole face at 4.90 m depth shows a relatively stable zone as consolidated rocks at this level have less signs of weakening.

Figure 10 shows photos of video-endoscopic survey of wellbore No. 4, during which the changes in the geomechanical state of the mass are recorded at different depths.

The wellbore No. 4 is also surveyed using video endoscopy to identify areas of rock weakening, the presence of caverns and to assess the overall geomechanical state of the mass at various depths. The initial area of the wellbore No. 4, corresponding to the wellhead (Fig. 10, *h* = 0.00 m), demonstrates a stable rock state with no visible signs of deformation or failure. After that, at a depth of 0.50 m, an inclined surface of weakening is fixed, indicating an increased local stresses and, as a consequence, a decrease in the mass stability.

Significant disturbance is recorded at a depth of 2.00 m, where there is a cavern. That is, there is a cavity zone in the rocks here. Further survey has revealed another zone of weakening at a depth of 5.90 m, which may be the result of ongoing fracture formation. At a depth of 8.70 m, a cavern is again noted. Its presence indicates the development of cavity structures in the rocks at greater depth, which increases the risk of wellbore deformation. At a depth of 9.40 m, a stable mass state is observed.

Figure 11 shows photos of video-endoscopic survey of wellbore No. 5, during which the changes in the geomechanical state of the mass are recorded at different depths.

Survey of the geomechanical state of wellbore No. 5 using video endoscopy indicates signs of rock cleavage, the presence of caverns and rock inclusions. The initial level, corresponding to the wellhead (Fig. 11, *h* = 0.00 m), is characterized by stable state of rocks without visible failure. The upper layers retain their continuity and are not exposed to significant deformation. At a depth of 1.10 m, the first signs of rock cleavage are recorded. Continuation of cleavage at a depth of 1.50 m indicates an increase in weakening processes, which reduces the strength of the mass at this level.

Depth of 3.40 m is characterized by the presence of a cavern, and at a depth of 3.70 m, there is a rock inclusion, presumably of ore origin.

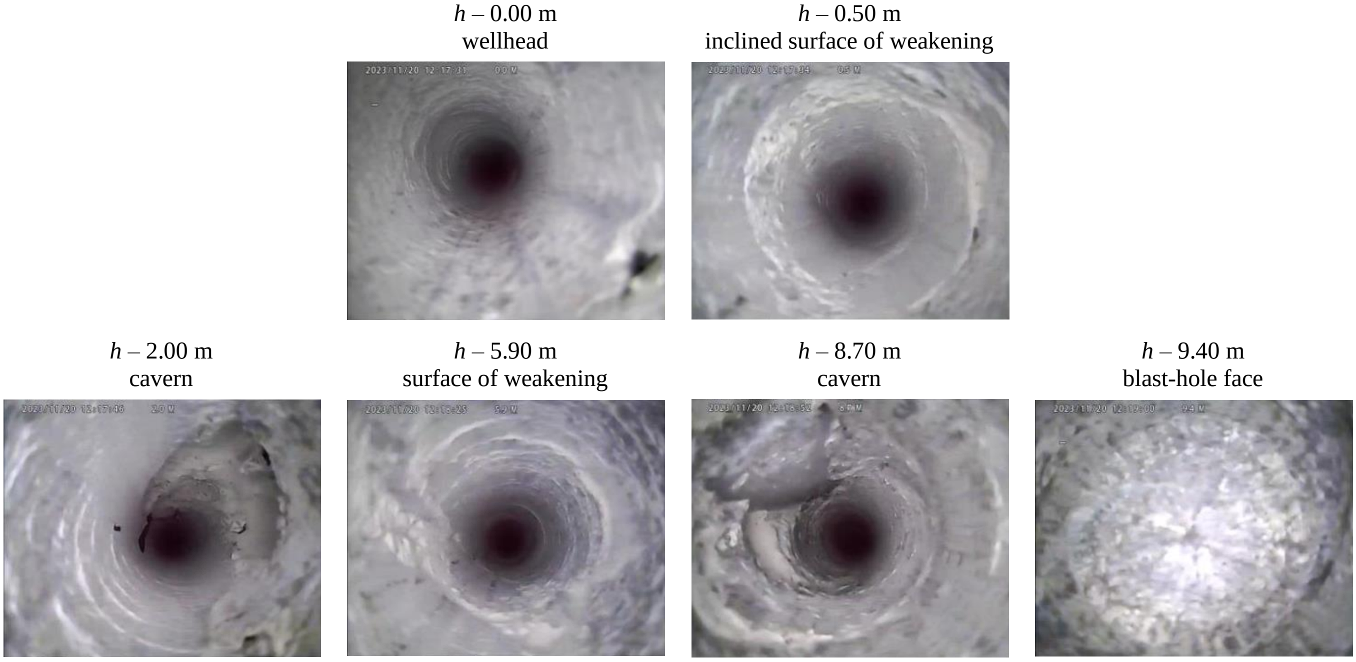

Figure 10. Survey of the wellbore No. 4 geomechanical state

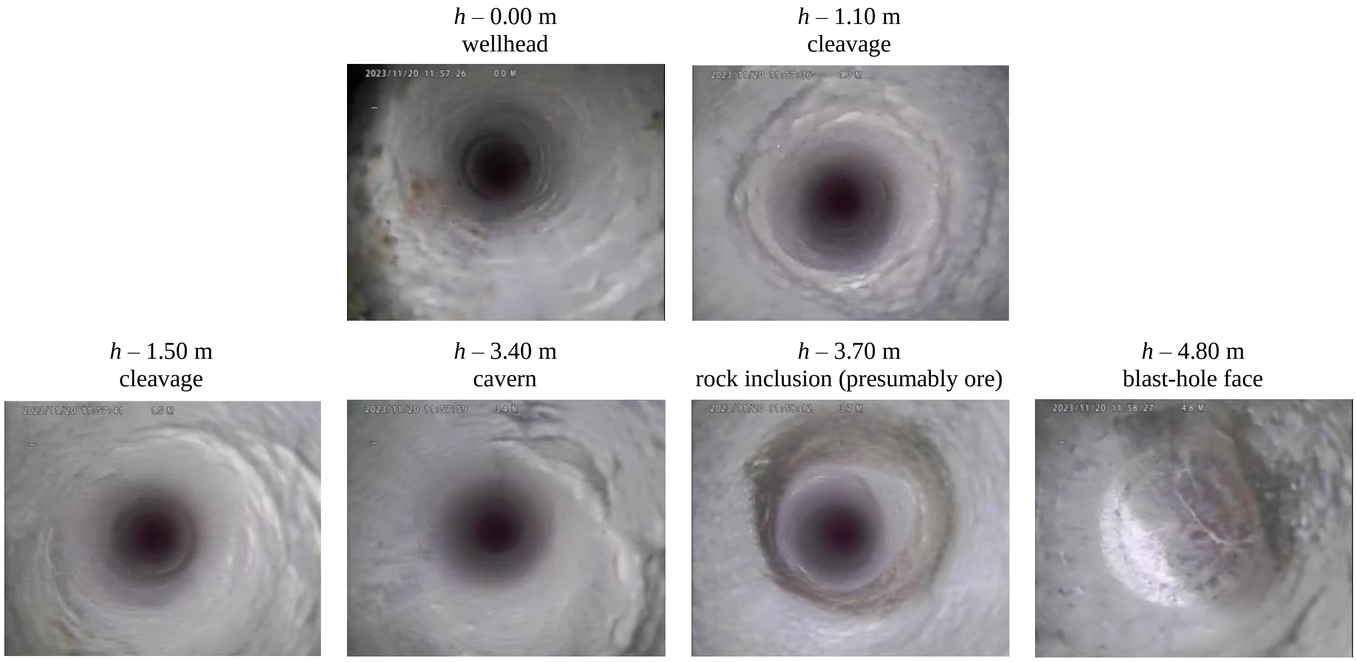

Figure 11. Survey of the wellbore No. 5 geomechanical state

The blast-hole face at a depth of 4.80 m demonstrates a more stable rock state. Consolidated layers at this level are compacted, which contributes to the improvement of the geomechanical state of the rock mass.

4.3. Control of rock displacement using reference depth markers (RDM)

To assess the rock mass stability, the research uses RDM to monitor the roof displacements. The control method provides for the setting of reference points in the key points of the experimental site with regular recording of changes in their position. Data obtained from the reference markers make it possible to determine the dynamics of displacements and assess the stability of the rock mass in the observation zone. Table 3 summarizes the results of roof rock displacement measurements at the experimental site, obtained during monitoring using RDM No. 1 and RDM No. 2.

The measurement results show a gradual increase in roof displacements during the observation period. At the site of RDM No. 1 for three and a half months, the maximum displacement has reached 7 mm, and the changes are uniform without sharp jumps, indicating the relative mass stability. The indicators are within the green zone, which indicates no critical deformation.

Similar dynamics is observed for RDM No. 2, where the maximum displacement is 5 mm. The displacement values also increase gradually, which confirms the rock mass stability at this site. Slight excess of displacements at individual points is within the permissible limits, which does not require urgent stabilization measures.

Table 3. Results of observations of roof rock displacements at the experimental site

Date of taking readings	R_1, mm	R_2, mm	R_3, mm	Notes
RDM No. 1				
01.08.2023	0	0	0	RDM setting
07.09.2023	2	3	4	Readings in the green zone
12.10.2023	3	3	5	
18.11.2023	5	4	7	
RDM No. 2				
07.10.2023	0	0	0	RDM setting
12.10.2023	3	3	5	Readings in the green zone
18.11.2023	4	5	5	

The obtained data lead to the conclusion that in the current mining-geological conditions the mass remains stable, and control over its state with the use of RDM provides rapid identification of possible changes. Further monitoring will make it possible to clarify the patterns of displacement development and, if necessary, to take measures to strengthen mine workings.

4.4. Assessment of support performance at the experimental site

At the experimental site of logistic drive No. 1 at hor. -175 m, a visual and instrumental survey was performed to assess the support performance. In the period from 25.07.2023 to 21.11.2023, when conducting mining operations at the experimental site of logistic drive No. 1 at hor. -175 m, two types of supporting – combined and active – were used. Combined support (1-15 m) consisting of roof-bolting support of the first level AKM20.01-AB (L = 2.4 m) set in the arch and sides of the mine working, deep-laid roof-bolting support AK01-21N(U) (L = 8.0 m) in the arch and AK01-21N(U) (L = 4.0 m) in the sides of the mine working. The first-level roof bolts are supported by flexible rope grips (PGK15 and PGK15A) and individual supporting elements (300×300×8 mm hemispherical support washer) for deep-laid roof-bolts. Welded lattice-like lacing with a mesh of 50×100 mm and bar thickness of 5 mm is used as a restraint for the arch and sides. Two layers of MasterROCK STS 1510 shotcrete with a total thickness of up to 100 mm are applied to the arch and sides of the experimental site. At the time of the survey, the experimental site of logistic drive No. 1 at hor. -175 m is supported according to the support pattern. DAC-1-500N resin capsules are used to fix roof bolts in the blast-holes. Additionally, for deep-laid roof-bolts AK01-21N(U), the blast-hole is completely filled with a bonding compound (two-component resin) in the amount of 15 liters per blast-hole (Figs. 12, 13).

Active support (16-30 m) consisting of roof-bolting support of the first level AKM20.01-AB (L = 2.4 m) set in the arch and sides of the mine working, deep-laid roof-bolting support VAU3 (AK01-30PN) (L = 8.0 m) in the arch of the mine working and VAU3 (AK01-30PN) (L = 4.0 m) in the sides of the mine working. The first-level roof bolts are supported by flexible rope grips (PGK15 and PGK15A) and individual supporting elements (300×300×8 mm hemispherical support washer) for deep-laid roof-bolts. Welded lattice-like lacing with a mesh of 50×100 mm and bar thickness of 5 mm is used as a restraint for the arch and sides.

Figure 12. Complete filling of the blast-hole with two-component resin

Figure 13. General view of the roof bolt after complete filling

Two layers of MasterROCK STS 1510 shotcrete with a total thickness of up to 100 mm are applied to the arch and sides of the experimental site. At the time of the survey, the experimental site of logistic drive No. 1 at hor. -175 m is supported according to the support pattern. DAC-1-500N resin capsules are used to fix roof bolts in the blast-holes. After setting the roof-bolts VAU3 (AK01-30PN), they are pre-tensioned axially by up to 100 kN, which is controlled by means of a deformation indicator.

During the first 15 m, the problem of stability of the unsupported mass arose, leading to the occurrence of rockfalls and dome formation in the bottom-hole space. To prevent further development of rockfalls and safe mining operations, a number of measures were taken. As a result of the measures taken, these rockfalls were eliminated, brought to a stable and safe state, and their further development was prevented.

List of measures taken:

1. During mining-tunneling operations in the unstable zone, the passport for drilling-blasting operations was adjusted (the length of blast-holes for drilling-blasting operations was reduced from 1.0 to 0.5 m, according to the recommendations of the DGOK geotechnical service), and the amount of explosive was reduced to 10 kg. After passing the unstable zone, the third passport for drilling-blasting operations was used with the blast-hole length of 1.0 m, but with a reduced amount of explosive relative to the first passport to 16 kg.
2. The step of setting the AKM 20.01-AB and AK01-21N(U) roof-bolting support rows was reduced from 1 to 0.8 m.

3. Additional resin-grouted rockbolts AKM 20.01-AB $L = 2.4$ m, additional rope bolts AK01- 21N(U) $L = 4.0$ m and 8.0 m, as well as additional sections of lattice-like lacing were set up in the places of rockfalls.

4. An additional 9 tons of shotcrete mixture was applied in the places of rockfalls.

4.5. Performance assessment of roof-bolting support

The roof-bolting support performance was assessed with the help of the rod puller PKA-3. Roof bolts of AK01-21N(U) and AKM20.01-AB types were tested, set to strengthen the support of the left side of the experimental site. The roof bolts were exposed to a load of 50% of the passport load-bearing capacity of the support. The test results are presented in Table 4. The tested roof bolts of AK01-21N(U) and AKM20.01-AB types have withstood the required load. The test results of the roof-bolting support (Table 4) confirm its performance under load application, which is 50% of the passport load-bearing capacity of the support. All tested roof bolts of AK01-21N(U) and AKM20.01-AB have withstood the specified loads without residual displacements, which indicates high efficiency of their setting and reliability of roof-bolting.

In this case, roof bolts of AK01-21N(U) type, set with two-component resin, have demonstrated different ultimate load depending on the stage of filling: before complete filling, the withstood load is 110 kN, and after complete filling it is 160 kN. Given improvements indicate a significant improvement in the load-bearing capacity of roof bolts after the resin injection process is completed, confirming the importance of high-quality roof-bolt hole filling to maximize the support performance.

The roof bolt AKM20.01-AB, set to strengthen the left side support, has withstood a load of 60 kN without displacement, which also confirms its compliance with the operational requirements. In general, the tests conducted show that the roof-bolting support used corresponds to the design parameters, providing sufficient stability of the mine workings in this area.

Table 4. Results of roof-bolting support performance testing

No.	Roof bolt type	Test location	Load on the support, kN	Displacement, mm
1	AK01-21N(u) until completely filled with two-component resin	32.65 m from MT-8417 (right side)	110	0
2	AKM20.01-AB	33.15 m from MT-8417 (left side)	60	0
3	AK01-21N(u) after completely filled with two-component resin	32.65 m from MT-8417 (left side)	160	0

4.6. Performance assessment of shotcrete support

The shotcrete support performance was assessed using non-destructive method instrumentally – shock-pulse method with the help of ONIKS 2.5 electronic sclerometer. Visual inspection was used to detect deformations, fractures and cleavage, and tapping was used to detect cavities.

To ensure the reliability and stability of shotcrete supports, a series of tests was conducted to determine the change in the strength characteristics of the material depending on the curing time. The main focus was to assess the compressive strength of shotcrete at different time intervals.

Tests were conducted using an impact loading method with consecutive recording of compressive strength (R, MPa) and deviations from the mean value (Δ, %). For each time interval, the average strength, standard deviation, and coefficient of variation were calculated to classify shotcrete into strength classes. Results of shotcrete strength testing are given in Table 5.

Analysis of the data in the table shows that the strength of shotcrete increases with increasing curing time. On the 10th day, the average compressive strength is 19.34 MPa, which corresponds to the B15strength class.

Table 5. Results of determining the strength of shotcrete (R) over time

Parameters / time	10 days		15 days		15-28 days		28 days	
Impact No.	R, MPa	Δ, %	R, MPa	Δ, %	R, MPa	Δ, %	R, MPa	Δ, %
1	20.4	5.2	21.1	-9.0	32.3	0.0	34.7	10.1
2	17.8	-8.7	24.8	7.3	30	-7.7	29.4	-6.1
3	18.6	-4.0	23.4	1.7	32.6	0.9	31.2	0.0
4	19.3	-0.2	23.5	2.1	30.4	-6.3	34.1	8.5
5	18.9	-2.3	22.2	-3.6	31.4	-2.9	29.2	-6.8
6	20.8	7.0	24	4.2	32.6	0.9	30.2	-3.3
7	18.3	-5.7	24.6	6.5	33.9	4.7	31.3	0.3
8	18.4	-5.1	23	0.0	31.7	-1.9	30.5	-2.3
9	20.1	3.8	21.4	-7.5	34.3	5.8	33.5	6.9
10	20.8	7.0	21.9	-5.0	32.9	1.8	27.5	-13.5
Average compressive strength (R), MPa	19.34		23		32.3		31.2	
Standard deviation (σ), MPa	1.11		1.30		1.38		2.32	
Coefficient of variation (V), %	5.73		5.66		4.27		7.43	
Strength class averaged	B15		B15		B25		B22.5	

On the 15th day, there is an increase in strength up to 23 MPa (class B15 on the border with B20), and by the period of 15-28 days, the strength reaches 32.3 MPa, which allows the material to be classified as class B25. The average compressive strength of shotcrete corresponds to the passport values.

The calculation of coefficient of variation (V) shows that the value remains within the range of 4.27-7.43%, indicating a sufficiently high homogeneity of the material. Graphical representation of the change in the strength of shotcrete from the number of impacts is presented in Figure 14, which provides a visual assessment of the dynamics of change in strength characteristics and confirms the steady increase in the strength of the material during the first 28 days.

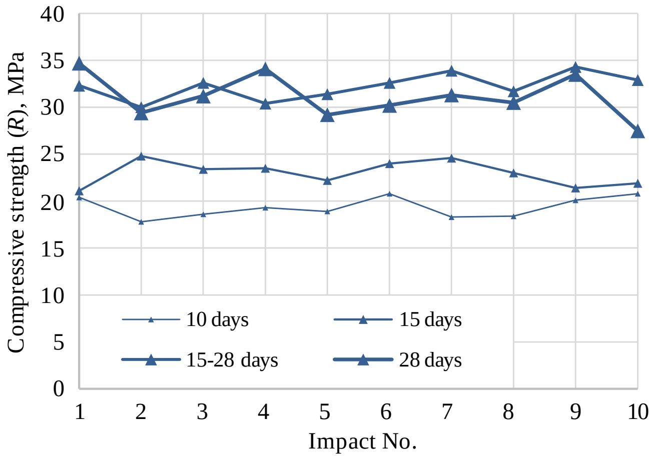

Figure 14. Graph of change in strength of shotcrete from the impact No. and time

To ensure the durability and stability of the shotcrete support, a series of tests were conducted to determine the strength characteristics of the material depending on the location along the length of the experimental site. Tests were performed on several key points (left and right sides) at different lengths: 0-10, 11-20 and 21-30 m. Determining the compressive strength (R, MPa) and deviation from the mean value (Δ, %) allows not only to assess the variations in strength characteristics, but also to classify shotcrete by strength in accordance with accepted standards. The test results are summarized in Table 6.

Analysis of the table shows that the strength of shotcrete varies depending on the sampling location. In the 0-10 m section, the average strength is 39.49 MPa, which corresponds to class B30. In the 11-20 m section, the strength decreases to 30.94-34.63 MPa, which corresponds to class B22.5. In the last section (21-30 m), the average strength stabilizes at 31.08-32.63 MPa level, which corresponds to class B22.5/B25.0. The graph of change in strength of shotcrete along the length of the experimental site is presented in Figure 15, where the dynamics of strength change for each test is visualized.

The coefficient of variation (V) varies in a range of 7.19-15.70%, indicating some scatter in the data, especially in the 21-30 m section. However, in general, the strength characteristics of shotcrete remain at an acceptable level, corresponding to the requirements for materials of this type.

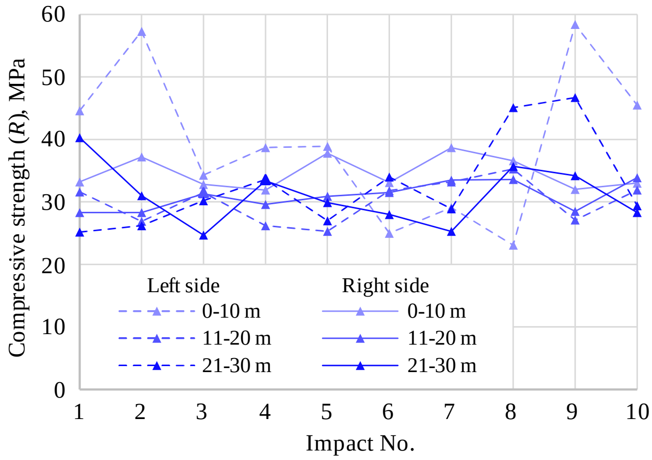

Figure 15. Graph of change in strength of shotcrete from the impact No. along the length of the experimental site

Table 6. Results of determination of shotcrete strength (R) and deviation (Δ) along the length of the experimental site

Parameters / location	0-10 m, left side		0-10 m, right side		11-20 m, left side		11-20 m, right side		21-30 m, left side		21-30 m, right side	
Impact No.	R, MPa	Δ, %	R, MPa	Δ, %	R, MPa	Δ, %	R, MPa	Δ, %	R, MPa	Δ, %	R, MPa	Δ, %
1	44.6	11.5	33.2	-4.3	31.6	4.8	28.3	-9.3	25.2	-29.5	40.3	22.9
2	57.3	31.1	37.2	6.9	26.9	-11.8	28.3	-9.3	26.2	-24.5	31	-0.3
3	34.3	-15.1	32.8	-5.6	31.5	4.5	31.3	1.2	30.2	-8.0	24.7	-25.8
4	38.7	-2.0	31.9	-8.6	26.2	-14.8	29.6	-4.5	33.6	2.9	33.4	6.9
5	38.9	-1.5	37.8	8.4	25.3	-18.9	30.9	-0.1	27	-20.9	29.9	-3.9
6	25	-58.0	33.1	-4.6	31.8	5.4	31.5	1.8	34	4.0	28	-11.0
7	29.1	-35.7	38.7	10.5	33.2	9.4	33.5	7.6	28.9	-12.9	25.3	-22.8
8	23.1	-71.0	36.6	5.4	35.3	14.8	33.6	7.9	45.1	27.6	35.7	12.9
9	58.4	32.4	32	-8.2	27.1	-11.0	28.5	-8.6	46.7	30.1	34.2	9.1
10	45.5	13.2	33	-4.9	31.9	5.7	33.9	8.7	29.4	-11.0	28.3	-9.8
Average compressive strength (R), MPa	39.49		34.63		30.08		30.94		32.63		31.08	
Standard deviation (σ), MPa	12.25		2.62		3.41		2.22		7.56		4.88	
Coefficient of variation (V), %	31.03		7.57		11.33		7.19		23.18		15.70	
Strength class averaged	B30		B25		B22.5		B22.5		B25.0		B22.5	

The results obtained are generally consistent with previously known data on the strength characteristics of shotcrete. The strength values in the range of 30-40 MPa and coefficients of variation in the range of 5-15% are consistent with the results of studies published in papers devoted to the assessment of shotcrete supports in mine workings [33]-[35]. The observed strength decrease in some sections confirms the conclusions about the influence of conditions of concrete application and curing on its strength properties.

Prospects for further research are related to the study of the influence of various factors on the strength characteristics of shotcrete, including the composition of the mixture, conditions of application and peculiarities of curing in mine conditions. Special attention should be paid to long-term changes in material strength, its fracture resistance and resistance to aggressive media. No less important direction is the development of methods to increase the homogeneity of concrete structure and to reduce the coefficient of variation, which will improve the performance characteristics of shotcrete support and increase its reliability in difficult mining-geologic conditions.

5. Conclusions

Video-endoscopic survey of wells has revealed the following: deformations of the border mass (fracture opening, cleavage) to a depth of 1.0-1.6 m (mainly in the roof). Numerous closed surfaces of weakening are observed throughout the depth of the studied site, intersecting the wells at various angles. The mass is characterized predominantly as homogeneous highly fractured, but in well No. 3 (20^{th} m of the experimental site) multiple dark-colored rock inclusions (presumably ore) are observed, which may act as areas of mass weakening during the mine working operation.

To increase the roof-bolting support performance and increase the border mass stability of the experimental site of logistic drive No. 1, by reinforcing after fixing the rope bolt AK01-21N (U), the blast-hole is completely filled with two-component resin in the amount of 15 liters per blast-hole. The complete filling of AKM20.01-AB (L = 2.4 m) is realized using DAK-1-500 N resin capsules.

When using the 2^{nd} scheme of supporting the experimental site of logistic drive No. 1, the increase in the support effectiveness is achieved by creating tension of the bearing rod of the rope bolt AK01-30PN (tensioning more than 50% of the rope bolt rod length) to the value of up to 100 kN. In addition to the rope bolts, the first level support AKM20.01-AB (L = 2.4 m) is used with complete filling of the blast-hole space with DAK-1-500 N resin capsules.

In addition to the roof-bolting support, a 100 mm thick shotcrete support of MasterRock STS 1510 is used. At the time of completion of tests at the experimental site, the average strength of the shotcrete ranges from 27.8 to 41.9 MPa (depending on aging), which corresponds to passport values. As of 20.11.2023, the shotcrete is in satisfactory condition. In local areas, there is a formation of hair-type fractures, extending from the protruding elements of the roof-bolting support, which is due to the difference in their deformation properties of the materials. There is no drummy sound when tapping the shotcrete. Further monitoring of the development of deformation processes in shotcrete support is required.

The indicators of the RDM measuring stations No. 1 and No. 2, previously set in the course of tunneling operations, testify to the absence of obvious deformations in the roof of the mine working. This is also confirmed by the results of a video-endoscopic survey of wells drilled near them.

Author contributions

Conceptualization: ZS, GI; Data curation: AA; Formal analysis: MI, KN, GI; Funding acquisition: GI; Investigation: AA, RO; Methodology: AA, GB; Project administration: ZS, KN; Resources: MI; Software: AA, GI; Supervision: GB; Validation: ZS, GI; Visualization: AA, KN; Writing – original draft: MI; Writing – review & editing: AA, RO, GB. All authors have read and agreed to the published version of the manuscript.

Funding

This research received no external funding.

Conflicts of interests

The authors declare no conflict of interest.

Data availability statement

The original contributions presented in the study are included in the article, further inquiries can be directed to the corresponding author.

References

[1] Kunarbekova, M., Yeszhan, Y., Zharylkan, S., Alipuly, M., Zhantikeyev, U., Beisebayeva, A., Kudaibergenov, A., Rysbekov, K., Toktarbay, Z., & Azat, S. (2024). The state of the art of the mining and metallurgical industry in Kazakhstan and future perspectives: A systematic review. *ES Materials & Manufacturing*, *25*, 1219. http://doi.org/10.30919/esmm1219

[2] Yelemessov, K.K., Baskanbayeva, D.D., & Sabirova, L.B. (2024). Optimization of technical means and technological processes of gas compression for the mining industry of the republic of Kazakhstan. *News of the National Academy of Sciences of the Republic of Kazakhstan, Series of Geology and Technical Sciences*, *5*, 36-46. https://doi.org/10.32014/2024.2518-170X.443

[3] Yussupov, K., Aben, E., Myrzakhmetov, S., Akhmetkanov, D., & Sarybayev, N. (2024). Increasing the efficiency of underground block leaching of metal. *Civil Engineering Journal*, *10*(10), 3339-3349. https://doi.org/10.28991/CEJ-2024-010-10-014

[4] Galiev, S.Zh., Uteshov, E.T., Galiev, D.A., & Farakhov, K.A. (2021). Methods and techniques for energy efficiency assessment of geotechnological facilities at opencast mines based on the in-depth analysis. *Eurasian Mining*, *35*(1), 65-69. https://doi.org/10.17580/em.2021.01.13

[5] Umarbekova, Z.T., Zholtayev, G.Z., Zholtayev, G.Z., Amralinova, B.B., & Mataibaeva, I.E. (2020). Silver halides in the hypergene zone of the arkharly gold deposit as indicators of their formation in dry and hot climate (Dzungar Alatau, Kazakhstan). *International Journal of Engineering Research and Technology*, *13*(1), 181-190. https://doi.org/10.37624/ijert/13.1.2020.181-190

[6] Safonov, A.A., Mausymbaeva, A.D., Portnov, V.S., Parafilov, V.I., & Korobko, S.V. (2019). Analysis of potential use of coal from the Shubarkol deposit in technical silicon smelting. *Ugol*, *2*, 68-72. https://doi.org/10.18796/0041-5790-2019-2-68-72

[7] Parafilov, V.I., Amangeldikyzy, A., Portnov, V.S., Kopobayeva, A.N., & Maussymbayeva, A.D. (2020). Geochemical specialization of the Shubarkol deposit coals. *Naukovyi Visnyk Natsionalnoho Hirnychoho Universytetu*, *5*, 5-10. https://doi.org/10.33271/nvngu/2020-5/005

[8] Uskenbayeva, R., Moldagulova, A., & Mukazhanov, N.K. (2020). Creation of data classification system for local administration. *Optimization of Complex Systems: Theory, Models, Algorithms and Applications*, 761-768. https://doi.org/10.1007/978-3-030-21803-4_76

[9] Turegeldinova, A., Amralinova, B., Fodor, M.M., Rakhmetullina, S., Konurbayeva, Z., & Kiizbayeva, Z. (2024). STEM and the creative and cultural industries: The factors keeping engineers from careers in the CCIs. *Frontiers in Communication*, *9*, 1507039. https://doi.org/10.3389/fcomm.2024.1507039

[10] Omarov, B., Baikuvekov, M., Sultan, D., Mukazhanov, N., Suleimenova, M., & Zhekambayeva, M. (2024). Ensemble approach combining deep residual networks and bigru with attention mechanism for classification of heart arrhythmias. *Computers, Materials & Continua*, *80*(1), 341-359. https://doi.org/10.32604/cmc.2024.052437
[11] Kalpeyeva, Z., Kassymova, A., Umarov, T., Mustafina, A., & Mukazhanov, N. (2020). The structure and composition of the business process model. *ACM International Conference Proceeding Series*, 1-6. https://doi.org/10.1145/3410352.3410783
[12] Satybaldiyeva, D., Mukhanova, G., Tymbayeva, Z., Tyshkanbayeva, M., & Bolatkyzy, S. (2023). Applying the expert method to determine a company's strategic goals. *Transport Problems*, *18*(2), 123-132. https://doi.org/10.20858/tp.2023.18.2.11
[13] Diomin, V.F., Khalikova, E.R., Diomina, T.V., & Zhurov, V.V. (2019). Studying coal seam bedding tectonic breach impact on supporting parameters of mine workings with roof bolting. *Naukovyi Visnyk Natsionalnoho Hirnychoho Universytetu*, *5*, 16-21. https://doi.org/10.29202/nvngu/2019-5/5
[14] Kyrgizbayeva, G., Nurpeisov, M., & Sarybayev, O. (2015). The monitoring of earth surface displacements during the subsoil development. *New Developments in Mining Engineering 2015: Theoretical and Practical Solutions of Mineral Resources Mining*, 161-167. https://doi.org/10.1201/b19901-30
[15] Kuldeev, E.I., Rysbekov, K.B., Donenbayevaa, N.S., & Miletenko, N.A. (2021). Modern methods of geotechnic – Effective way of providing industrial safety in mines. *Eurasian Mining*, *36*(2), 18-21. https://doi.org/10.17580/em.2021.02.04
[16] Sassykova, L., Sendilvelan, S., & Aubakirov, Y. (2019). Metal block catalysts for complex cleaning of harmful emissions of transport and the industry. *News of the National Academy of Sciences of the Republic of Kazakhstan, Series of Geology and Technical Sciences*, *4*(436), 12-23.
[17] Matayev, A.K., Musin, A., Abdrashev, R.M., Kuantay, A.S., & Kuandykova, A.N. (2021). Substantiating the optimal type of mine working fastening based on mathematical modeling of the stress condition of underground structures. *Naukovyi Visnyk Natsionalnoho Hirnychoho Universytetu*, *3*, 57-63. https://doi.org/10.33271/nvngu/2021-3/057
[18] Arystan, I.D., Nemova, N.A., Baizbaev, M.B., & Mataev, A.K. (2021). Efficiency of modified concrete in lining in underground structures. *IOP Conference Series. Earth and Environmental Science*, *773*(1), 012063. https://doi.org/10.1088/1755-1315/773/1/012063
[19] Imashev, A.Zh., Sudarikov, A.E., Musin, A.A., Suimbayeva, A.M., & Asan, S.Yu. (2021). Improving the quality of blasting indicators by studying the natural stress field and the impact of the blast force on the rock mass. *News of the National Academy of Sciences of the Republic of Kazakhstan*, *4*(448), 30-35. https://doi.org/10.32014/2021.2518-170x.78
[20] Lozynskyi, V., Yussupov, K., Rysbekov, K., Rustemov, S., & Bazaluk, O. (2024). Using sectional blasting to improve the efficiency of making cut cavities in underground mine workings. *Frontiers in Earth Science*, *12*, 1366901. https://doi.org/10.3389/feart.2024.1366901
[21] Zeitinova, S., Imashev, A., Bakhtybayev, N., Matayev, A., Mussin, A., & Yeskenova, G. (2024). Numerical modeling the rock mass stress-strain state near vertical excavations in combined mining. *Civil Engineering Journal*, *10*(9), 2919-2934. https://doi.org/10.28991/CEJ-2024-010-09-010
[22] Bazaluk, O., Petlovanyi, M., Zubko, S., Lozynskyi, V., & Sai, K. (2021). Instability assessment of hanging wall rocks during underground mining of iron ores. *Minerals*, *11*(8), 858. https://doi.org/10.3390/min11080858
[23] Bazaluk, O., Ashcheulova, O., Mamaikin, O., Khorolskyi, A., Lozynskyi, V., & Saik, P. (2022). Innovative activities in the sphere of mining process management. *Frontiers in Environmental Science*, *10*, 878977. https://doi.org/10.3389/fenvs.2022.878977
[24] Shustov, O.O., Pavlychenko, A.V, Bielov, O.P., Adamchuk, A.A., & Borysovska, O.O. (2021). Calculation of the overburden ratio by the method of financial and mathematical averaged costs. *Naukovyi Visnyk Natsionalnoho Hirnychoho Universytetu*, *5*, 30-36. https://doi.org/10.33271/nvngu/2021-5/030
[25] Shaldarbekov, K., Mukhanova, G., Dossova, S., Nurmukhambetova, Z., Mussaeva, G., & Shaldarbekova, K. (2018). Regional projects selection based on multi-criteria evaluation. *Journal of Advanced Research in Law and Economics*, *9*(6(36)), 2026-2034. https://doi.org/10.14505/jarle.v9.6(36).16
[26] Nurpeissova, M., Bekbassarov, S., Bek, A., Kyrgizbaeva, G., Turisbekov, S., & Ormanbekova, A. (2017). The geodetic monitoring of the engineering structures stability conditions. *Journal of Engineering and Applied Sciences*, *12*(11), 9151-9163. https://doi.org/10.3923/jeasci.2017.9151.9163
[27] Nurpeisova, M.B., Sarybaiev, O.A., & Kurmanbaiev, O.S. (2016). Study of regularity of geomechanical processes development while developing deposits by the combined way. *Naukovyi Visnyk Natsionalnoho Hirnychoho Universytetu*, *4*, 30-36.
[28] Polo Salinas, J., Marquina Araujo, J.J., & Cotrina Teatino, M.A. (2024). Uncertainty in underground mining operations: a bibliometric and systematic literature review analysis. *World Journal of Engineering*. Article in press. https://doi.org/10.1108/WJE-07-2024-0388
[29] Wang, Y., Fu, G., Lyu, Q., Wu, Y., Jia, Q., Yang, X., & Li, X. (2022). Reform and development of coal mine safety in China: An analysis from government supervision, technical equipment, and miner education. *Resources Policy*, *77*, 102777. https://doi.org/10.1016/j.resourpol.2022.102777
[30] Matayev, A.K., Kainazarova, A.S., Arystan, I.D., Abeuov, Ye., Kainazarov, A.S., Baizbayev, M.B., Demin, V.F., & Sultanov, M.G. (2021). Research into rock mass geomechanical situation in the zone of stope operations influence at the 10th Anniversary of Kazakhstan's Independence mine. *Mining of Mineral Deposits*, *15*(1), 103-111. https://doi.org/10.33271/mining15.01.103
[31] Sultanov, M.G., Mataev, A.K., Kaumetova, D.S., Abdrashev, R.M., Kuantay, A.S., & Orynbayev, B.M. (2020). Development of the choice of types of support parameters and technologies for their construction at the Voskhod field. *Ugol*, *10*, 17-21. https://doi.org/10.18796/0041-5790-2020-10-17-21
[32] Arystan, I.D., Baizbaev, M.B., Mataev, A.K., Abdieva, L.M., & Bogzhanova, Z.K. (2020). Selection and justification of technology for fixing preparatory workings in unstable massifs on the example of the mine "10 years of Independence of Kazakhstan. *Ugol*, *6*, 10-14. https://doi.org/10.18796/0041-5790-2020-6-10-14
[33] Bondarenko, V., Kovalevska, I., Sheka, I., & Sachko, R. (2023). Results of research on the stability of mine workings, fixed by arched supports made of composite materials, in the conditions of the Pokrovske Mine Administration. *IOP Conference Series: Earth and Environmental Science*, *1156*(1), 012011. https://doi.org/10.1088/1755-1315/1156/1/012011
[34] Sotskov, V., & Saleev, I. (2013). Investigation of the rock massif stress strain state in conditions of the drainage drift overworking. *Annual Scientific-Technical Collection – Mining of Mineral Deposits*, 197-201. https://doi.org/10.1201/b16354-35
[35] Bulat, A.F., Krukovskyi, O.P., & Krukovska, V.V. (2024). Deformation of gas-bearing rocks and gas filtration during excavation of mine workings. *International Applied Mechanics*, *60*(1), 10-19. https://doi.org/10.1007/s10778-024-01259-9

Розробка та впровадження активних і комбінованих типів кріплення на ділянках гірничих виробок, схильних до дії опорного тиску

А. Абдрашит, Ж. Саркулова, М. Імангазін, Р. Оразбекова, Г. Ісенгалієва, К. Науризова, Г. Бімагамбетова

Мета. Розробка та обґрунтування ефективної технології кріплення гірничих виробок в умовах складних геомеханічних і гідрогеологічних факторів на основі аналізу даних про деформаційний стан приконтурного масиву, ефективності застосовуваних кріплень, а також поведінки матеріалів та конструкцій у процесі експлуатації.

Методика. Дослідження включає використання ендоскопічної зйомки свердловин для діагностики приконтурного масиву з метою виявлення тріщин, розшарувань та інших зон ослаблення. Випробування проводилися на анкерному кріпленні, включаючи канатні анкери АК01-21Н(У) і АК01-30ПН з натягом до 100 кН. Для повного заповнення шпурів застосовувалися двокомпонентна смола (15 л на шпур) та полімерні ампули ДАК-1-500Н. Крім того, проводилося вивчення властивостей торкретбетонного кріплення марки MasterRock STS 1510 з контролем міцності динаміки.

Результати. Виявлено деформацію приконтурного масиву, включаючи розкриття тріщин до 1.6 м, викликані наявністю рудних включень. Застосування анкерного кріплення з повним заповненням шпурів двокомпонентною смолою та полімерними ампулами показало високу ефективність. Канатні анкери АК01-30ПН із натягом до 100 кН забезпечили значне підвищення стійкості масиву. Торкретбетон марки MasterRock STS 1510 продемонстрував задовільні характеристики міцності. Зафіксовано незначні тріщини, які не впливають на загальну стійкість виробок.

Наукова новизна. Виявлено та охарактеризовано закономірності деформаційної поведінки приконтурного масиву в умовах складних геомеханічних факторів, включаючи зони тріщинуватості й локальні ослаблення, зумовлені рудними включеннями. Встановлено, що повне заповнення шпурів двокомпонентною смолою та полімерними ампулами для армування канатних анкерів забезпечує значне підвищення стійкості масиву. Комплексне використання анкерного та торкретбетонного кріплення довело ефективність зниження впливу водопритоків і підвищення міцнісних характеристик виробок.

Практична значимість. Розроблена технологія кріплення гірничих виробок із використанням канатних анкерів з натягом до 100 кН та повним заповненням шпурів двокомпонентною смолою може бути впроваджена на гірничодобувних підприємствах, що підвищить стійкість виробок і безпеку робіт в умовах складних геомеханічних факторів. Результати ендоскопічної діагностики та моніторингу деформацій приконтурного масиву надають інструмент для своєчасного виявлення зон ослаблення та вжиття заходів щодо посилення кріплення, сприяючи підвищенню ефективності експлуатації гірничих виробок.

Ключові слова: *напружений стан, масив, руда, порода, свердловина, кріплення, Q-індекс Бартона*

Publisher's note

All claims expressed in this manuscript are solely those of the authors and do not necessarily represent those of their affiliated organizations, or those of the publisher, the editors and the reviewers.